

Technology Guide for Cryogenic RF switches



Definitions

ZC: System's characteristic impedance (Ω)

P: Power in watts

RAMSES : RAdiall Modular System for Electromechanical Switches

QuBits: Quantum bits

He : Helium

OFHC : Oxygen Free High Conductivity

RRR : Residual Resistivity Ratio

NbTi : Niobium Titanium

PCB : Printed Circuit Board

SEM : Scanning Electron Microscopy

Introduction to quantum computing

Radiall is working to customize and optimize RF switches for use in cryogenic cooling systems to support quantum computing. Quantum computing will revolutionize our understanding of the world by analyzing datasets that today's most powerful supercomputers can't handle. Instead of bits, quantum computers use qubits which can only be detected at extremely small energy levels and at temperatures close to absolute zero.

This requires cryogenic refrigeration systems with multiple stages of cooling and numerous RF cables of significant length. Radiall coaxial cryogenic switches, mounted at different temperature stages of the cryogenic chamber, help to switch several RF paths into cryogenic cooling systems.

Switch application

The unique design of RAMSES is based on the suppression of friction, in order to improve reliability and avoid electric contact and RF characteristics degradation.

In general, traditional switches operate by moving a rectangular section contact reed inside a rectangular cavity. These contact reeds are linked to dielectric material “transmission pushers” and directed by guides made of insulated material. During the switching sequences, these dielectric parts rub against the reeds and in the transmission holes, and generate insulating particles in the RF cavity that pollute the contacts, ultimately causing running defects and an increase in insertion. Figure 1 illustrates the build-up of minute dielectric particles on a set of conventional switch contacts after one million cycles.

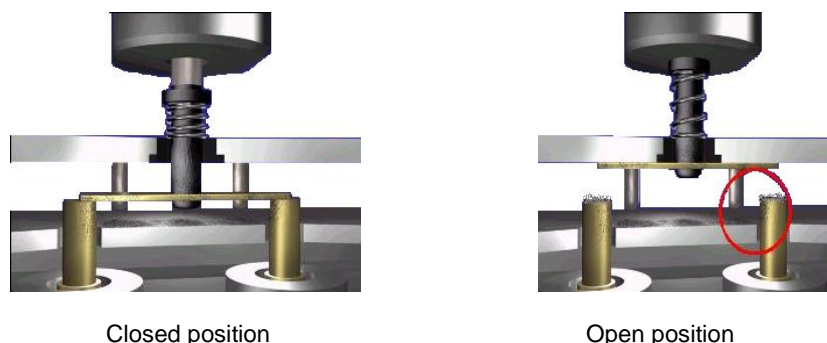


Figure 1 : Conventional switch contacts after one million cycles.

To eliminate this problem, all RAMSES devices incorporate the same modular patented system comprised of parallel spring blades suspended from a barrier located outside of the RF body. These blades create a rectilinear motion on the pusher. As a result, both friction and the production of particles inside and outside of the RF cavity are suppressed. Figure 2 shows a cutaway view of a patented RAMSES coaxial switch kinematics.

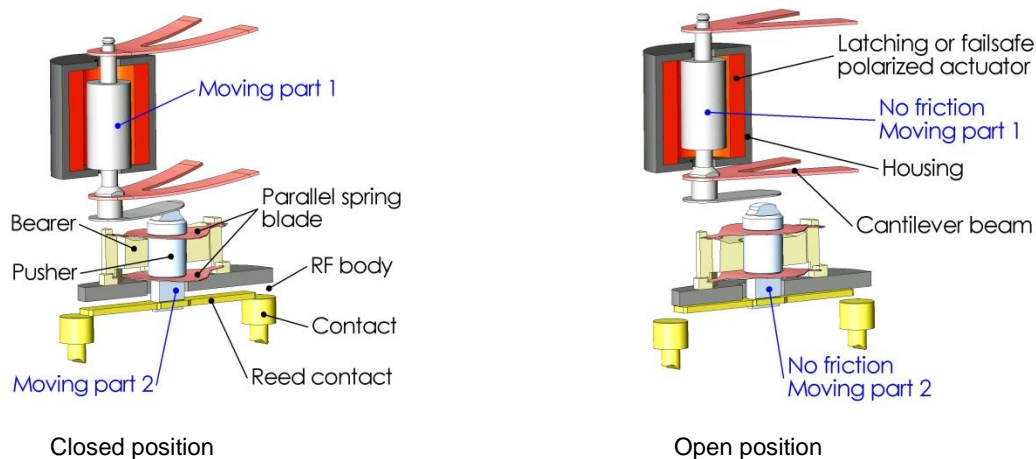


Figure 2 : RAMSES switch kinematics

The patented RAMSES polarized linear actuator has been manufactured for several years by Radiall. The miniature design uses high-energy magnets, and can be incorporated in both failsafe and latching models. The actuator produces a locking force and above all, contact forces that far exceed those of traditional actuators, resulting in a power consumption of few Watts. Figure 3 shows a cutaway view of a patented RAMSES polarized linear actuator.

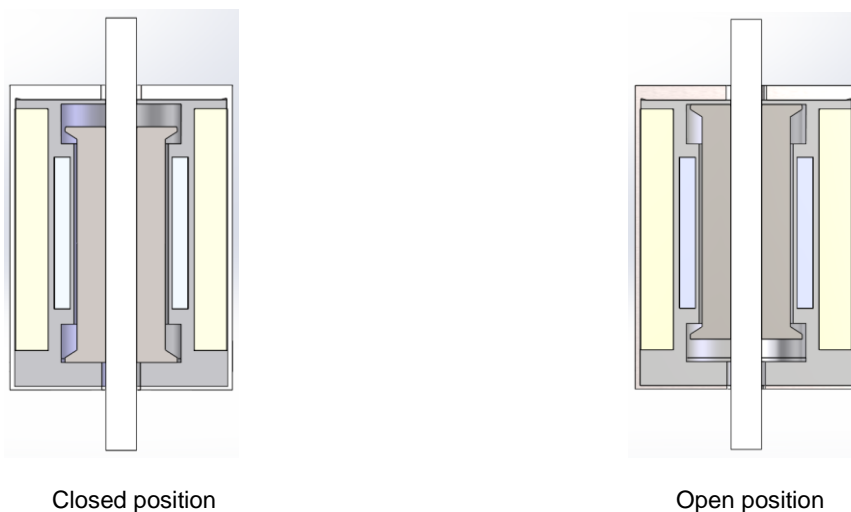


Figure 3 : Patented RAMSES polarized linear actuator

Figure 4 illustrates a cutaway view of the magnetic field for both positions. The system is used in the production of both failsafe and latching actuators, depending on how it is applied in the switch. These patented actuators have locking forces when coil is energized of 800g.

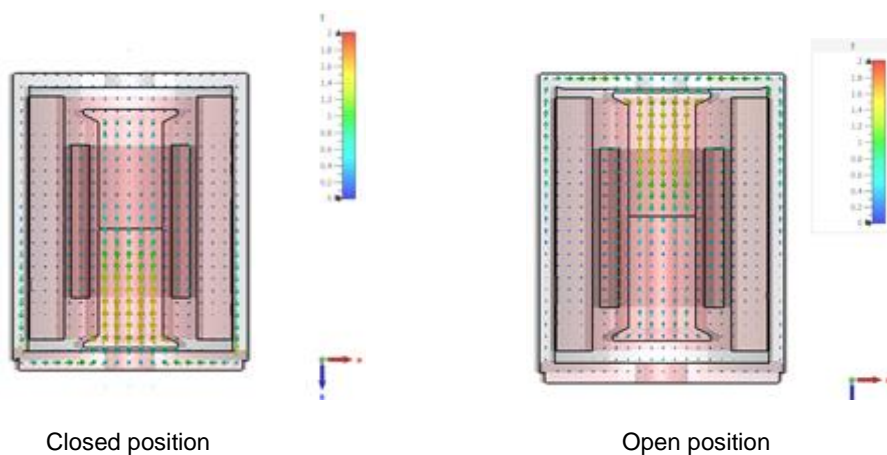


Figure 4 : Patented RAMSES polarized linear actuator magnetic field

Figure 5 shows the relationship between locking forces and position of polarized actuator with and without current.

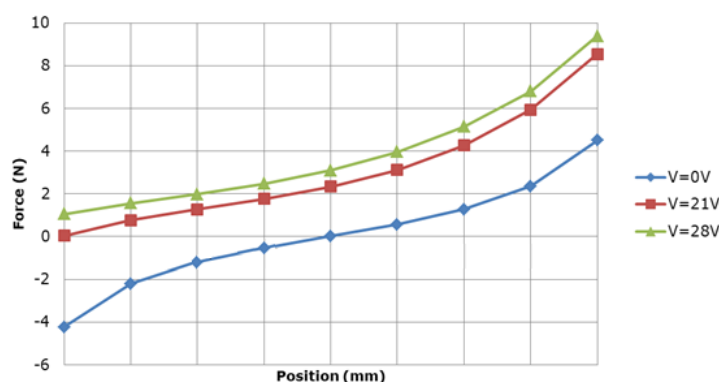


Figure 5 : Relation between locking forces and position of polarized actuator with and without current.

The actuator has the advantage of very low magnetic leakage, allowing actuators to be used close to the proximity to one another magnetic source without any degradation of performance. Figure 6 shows the integration of Radiall cryogenic switches inside dilution refrigerator. Close to RF switches bobbin with magnetic strength more than 1 Tesla is used.

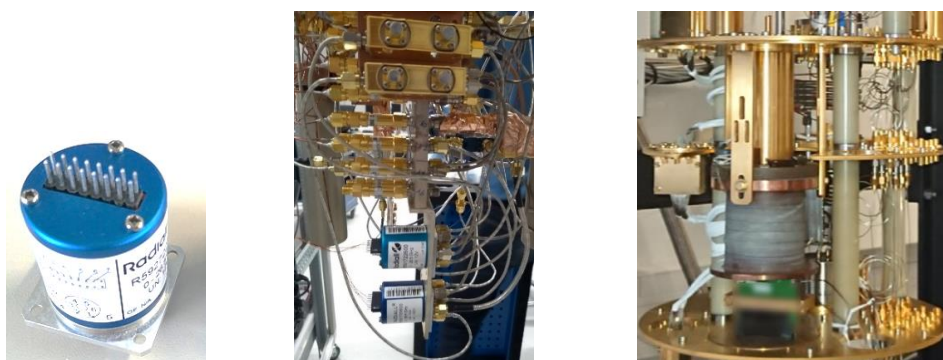


Figure 6 : Cryogenic switches inside dilution refrigerator.

Maximum magnetic field of 0.75mT is present at the surface of the anodized cylindrical cap. The field decays to 30μT at 1cm. It's possible that the cap turns superconducting below 1K and shields a large fraction of the stray field.

Specific features for cryogenic use

In the aim to avoid bad a connection at cryogenic temperature all solenoid pins are solder directly to the printed circuit board. The pushpin receptacles which could be fail at temperatures close to absolute zero are removed. In addition, for reliability at cryogenic temperature there is no PCB to PCB internal connection. Figure 7 illustrates the main parts of the cryogenic RAMSES SP6T switch.

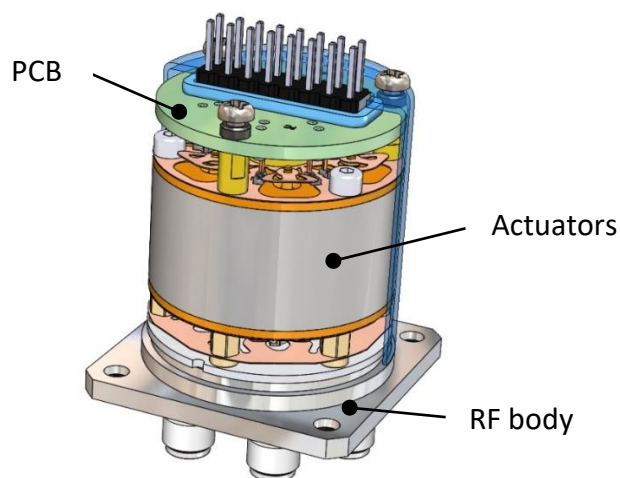
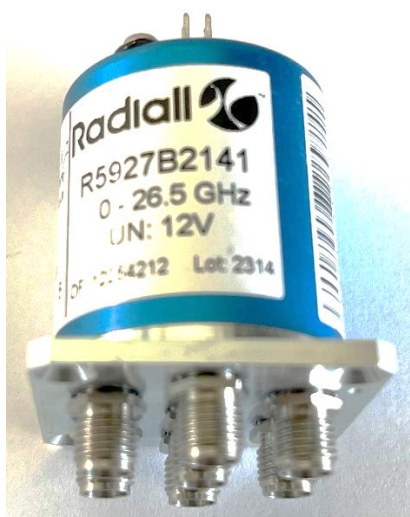


Figure 7 : Main parts of cryogenic RAMSES switches.

Electromechanical latching switches without any options contain a mechanism that will maintain a chosen RF contact path whether the voltage is maintained or not after switching is accomplished. A simple pulse duration equal to the maximum switching time is enough to change the switch position.

For example, on latching SP6T fitted with SMA type connectors the nominal coil resistance is 60 Ω at ambient temperature. The nominal operating current is 200mA at 23°C. Figure 8 shows the electrical characteristics of a non-cryogenic RF switch.

Operating mode	Latching
Nominal operating voltage (Vdc) (across operating temperature range)	12 (10.2 / 13)
Coil resistance (+/-10%) (Ohms)	60
Nominal operating current at 23°C (mA)	200

Figure 8 : Electrical characteristics of none cryogenic RF switch.

To close the desired RF path, ground must be applied to pin "-C" and power supply must be applied to corresponding "drive" pin. To open the paths, complete the operation by applying power supply to "reset" pin. Figure 9 illustrates the electrical schematic of non-cryogenic RF switch.

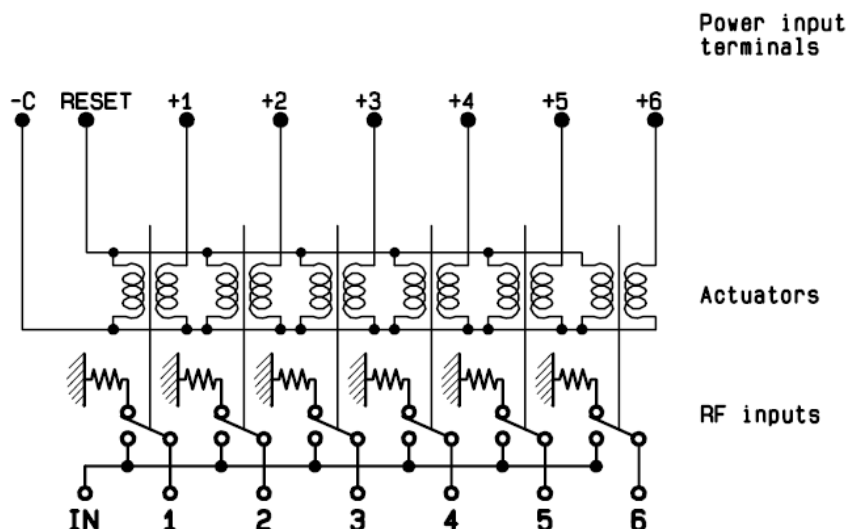


Figure 9 : Electrical schematic of none cryogenic RF switch.

To reduce impact on system temperature, set and reset coil of each actuator are in series on Radiall cryogenic switches. The same magnetic field can be applied with half current. Reset can be accomplished by reversing the direction of the current in the circuit. It limits the heating of the coils which is linked to a higher current value at low temperature. Figure 10 illustrates the electrical schematic of a Radiall cryogenic RF switch.

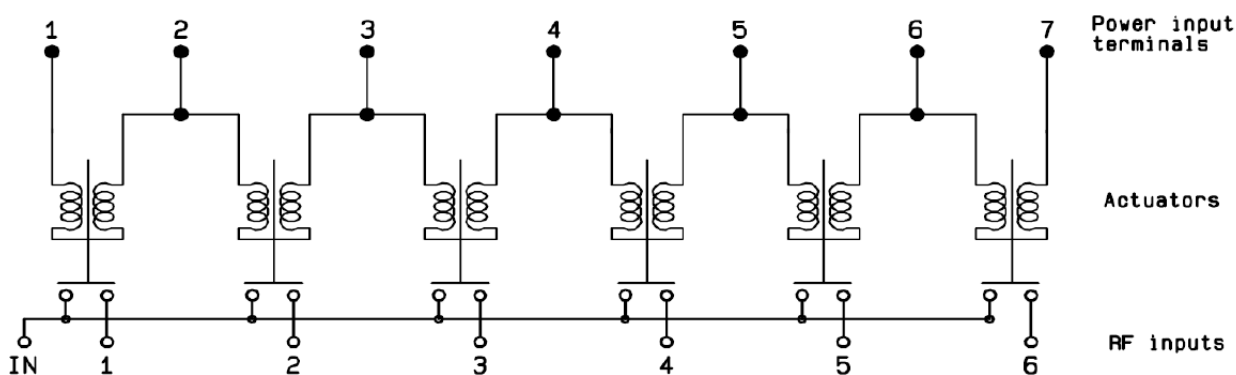


Figure 10 : Electrical schematic of Radiall cryogenic RF switch.

Using both set and reset solenoids in series the power dissipation is divided by 2. Figure 11 shows the power consumption between standard and cryogenic Ramses switches.

	Standard Ramses switch	Cryogenic Ramses switch
60 Ω per solenoids		
$P = U^2/R$	$12^2/60 = 2.4W$	$12^2/120 = 1.2W$

Figure 11 : Shows the power consumption between standard and cryogenic Ramses switch.

In addition, lesser voltage can be used to drive the same current through the circuit and the dissipation at low temperatures is much less.

DC resistance of standard and special coils used in RF switches

Three type of resistance were evaluated for coils at cryogenic temperature. The aim was to extract resistance variation versus temperature. Three coils made of said “normal copper”, “oxygen free copper”, and of superconducting NbTi in copper were measured and evaluated.

First of all, the superconducting wire used into coil actuators is composed by only one metallic strand of NbTi coated with a layer of copper. Figure 12 illustrate the SEM measurements of NbTi wire.

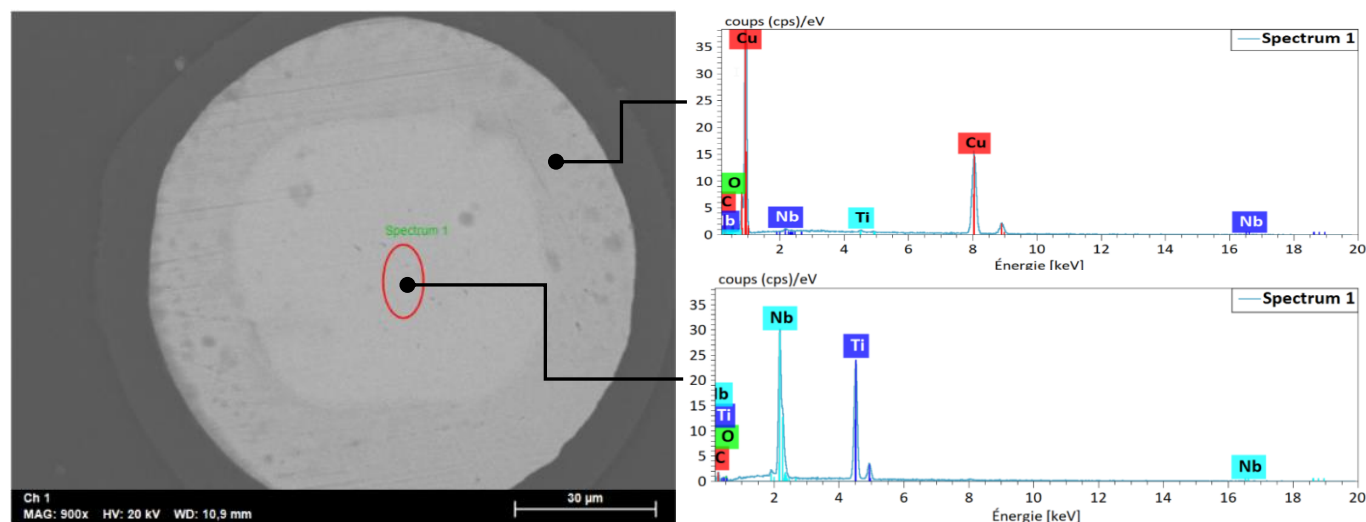


Figure 12 : SEM measurements of NbTi wire.

The setup is used to measure the temperature dependence of the coils DC resistance utilized a calibrated 0-300K thermometer and 4 wires measurement. Each coil is protected from water condensation by scotch tape. The head is plunged in liquid Helium and then raised slowly until the He vapors above the liquid. The resistance as well as the temperature are recorded during the temperature rise. Figure 13 shows pictures of the test method.

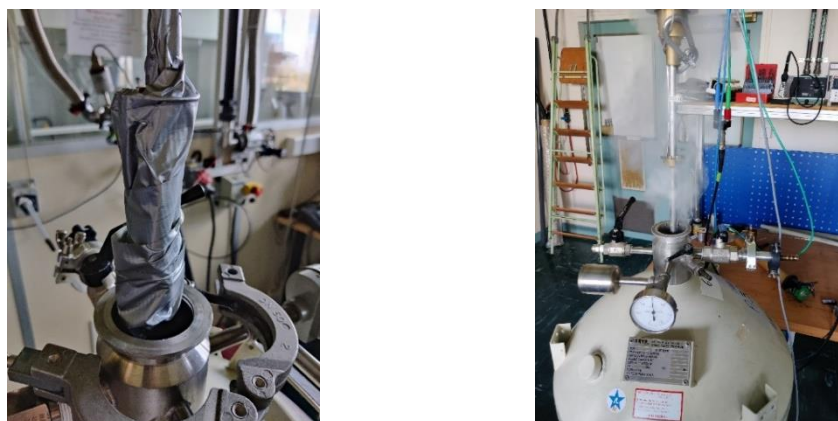


Figure 13 : Head protected with scotch tape plunged in a liquid Helium.

Then, the two copper coils (said “normal copper” and “OFHC”) showed a very similar resistance, decreasing from 63Ω at room temperature down to 0.55Ω below 10K . The residual resistivity ratio (RRR) of 102 is observed. This is typical of technical copper.

The NbTi-Cu coil have an 83Ω resistance at room temperature, it decreases down to 0.52Ω just before its superconducting transition at 8K , and then dropping to zero (less than $0.4\text{ m}\Omega$ measured). Figure 14 shows the resistance variation versus temperature for each coil.

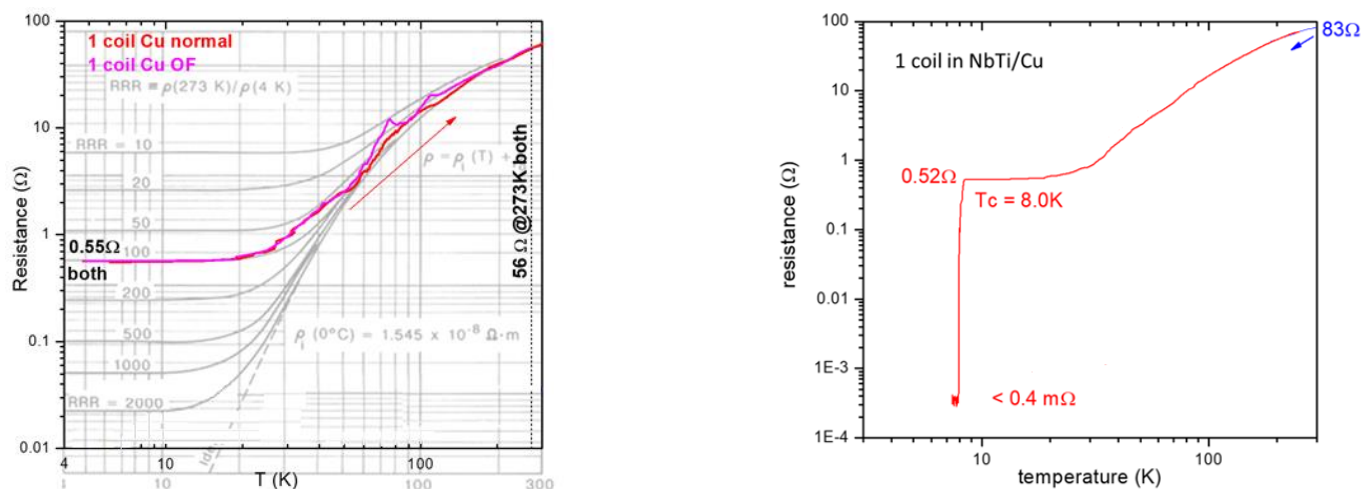


Figure 14 : Resistance variation vs temperature for each coil.

Switching pulse amplitude and duration at room temperature

We have determined approximately the appropriate nominal pulse current, duration and dissipated Joule energy to switch reliably with several SP6T switches placed either at room temperature.

The success probability is then plotted as a function of the pulse duration and current. The plot is complemented by iso-nominal pulse Joule energy lines (not taking into account the mechanical energy of the actuator in the switch).

Figure 15 shows the results for a SP6T with normal copper coils tested at room temperature. Region of 100% success (yellow) follow approximately iso- Joule energy lines (although it is slightly unfavorable to use short intense pulse rather than long-less intense ones).

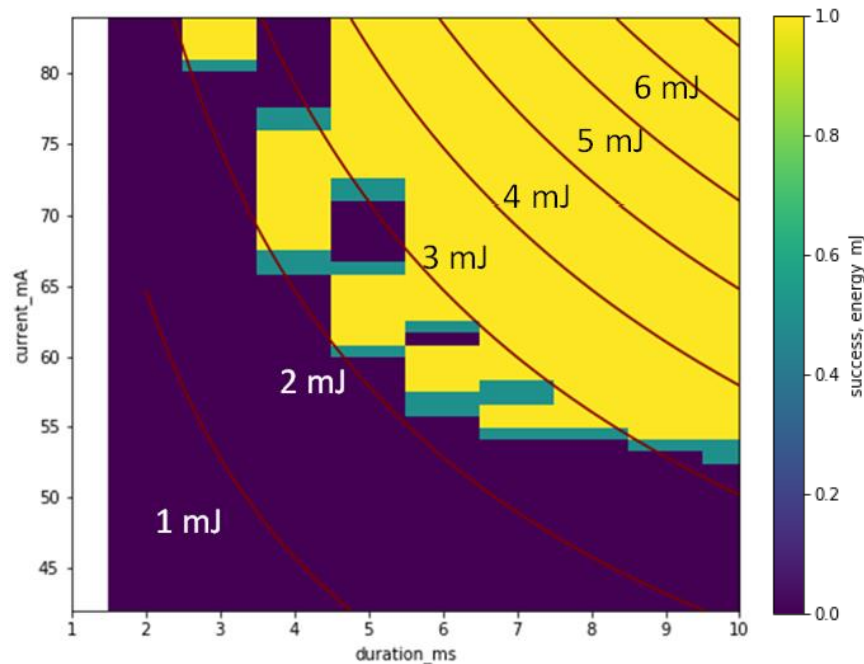


Figure 15 : Success probability at room temperature. Normal copper coils.

10 switching attempts were performed to compute a success probability. At room temperature, to close or open RF paths the switch needs 4mJ between 5 and 10ms.

Switching pulse amplitude and duration at 4.5K

We then compared the switching parameters at cryogenic temperature with those at room temperature in a new measurement round in a dilution refrigerator cooled. The switching current and durations are the same no matter what the operating temperature is. On the contrary, the pulse Joule energy is 110 times slower ($50\mu\text{J}$ vs 5.5 mJ) at low temperature.

The success probability is then plotted as a function of the pulse duration and current. The plot is complemented by iso-nominal pulse Joule energy lines (not taking into account the mechanical energy of the actuator in the switch). Figure 16 shows the results for a SP6T with normal copper coils tested at room temperature and at 4.5K. Region of 100% success follow approximately iso-Joule energy lines are drawn in cyan although it is slightly unfavorable to use short intense pulse rather than long-less intense ones.

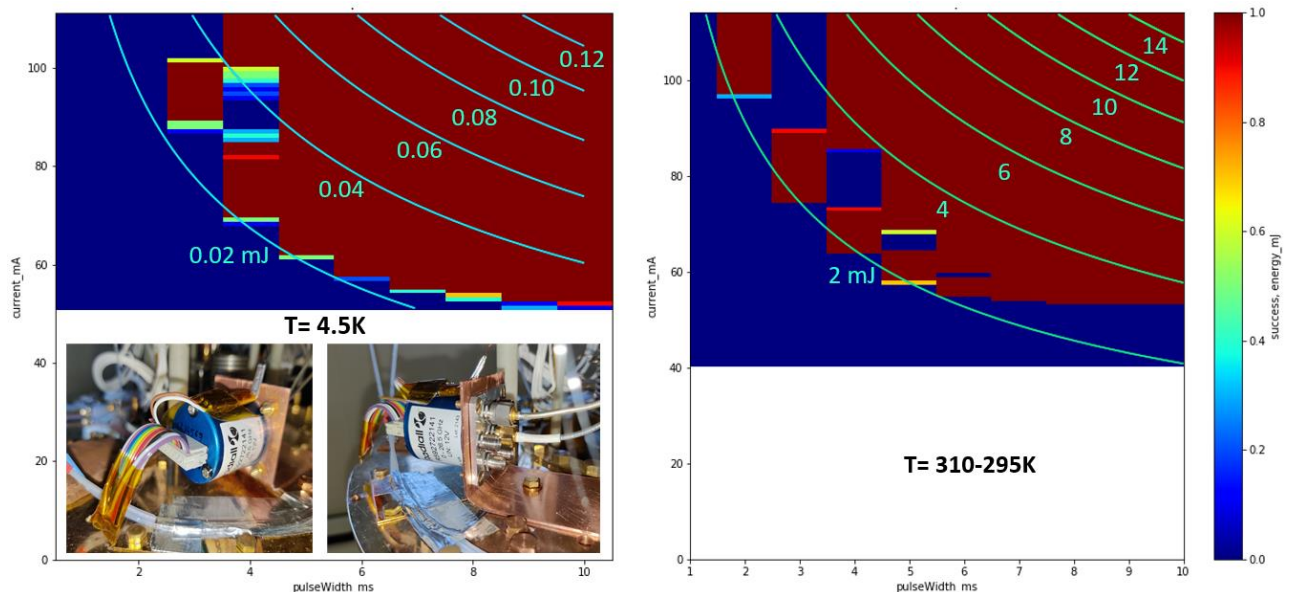


Figure 16 : Success probability at room temperature and 4.5K. Normal copper coils.

Energy dissipated at this working point is $40\mu\text{J}$ for normal copper coils at dilution temperature. Switching thermal impact will be visible in most dilution refrigerators but recoverable in minutes. NbTi coils should completely solve the thermal impact of a switching event.

Switching pulse amplitude and duration at 50mK

The heating of a dilution refrigerator induced by the switching of different SP6T was measured. The aim was to measure the impact of actuations close to absolute zero. The refrigerator is then cooled down at cryogenic temperature near 50mK. Figure 17 shows the results of the heating due to 7 close-open cycles (14 actuations) performed on SP6T fitted with normal copper coils every 2 seconds. The temperature of the base plate rises from T_{eq} 50mK up to 72 mK in less than 26s and then decays in a few hours back to T_{eq} .

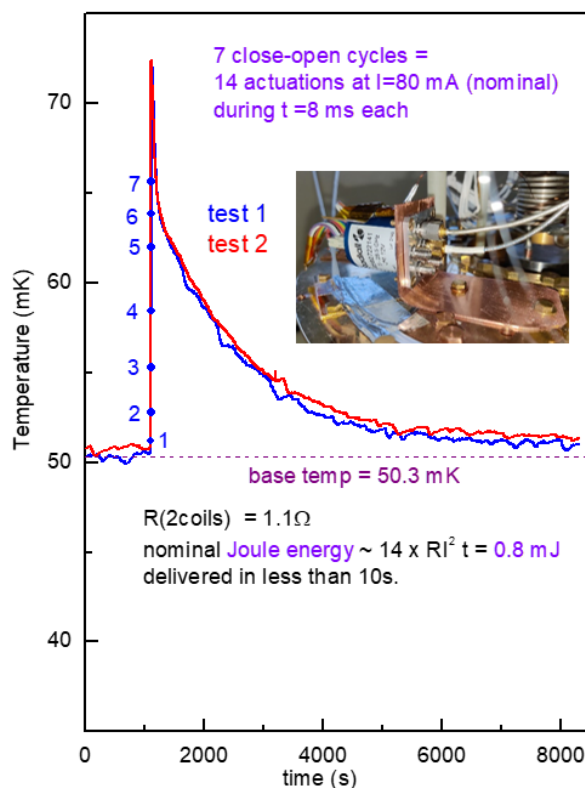


Figure 17 : Heating due to 7 close open cycles at 50mK. Normal copper coils.

The 0.8mJ Joule energy of the 14 pulses represents less than 7% of the about 12 mJ dissipated in total. This indicates that Joule dissipation in the coil resistance is far from being the main source of dissipation.

The interpretation of this result is that the inductive energy of the coil being transferred to the mechanical energy of the actuator (solid friction and kinetic energy) at a level of about 0.8mJ per actuation (12mJ/14 actuations).

We have also performed this type of measurement with an RF switch fitted with NbTi-Cu coils undergoing the same 7 close-open cycles as before, and with this same switch fed with 14 open pulses starting from the open state. Figure 18 shows the results compiled.

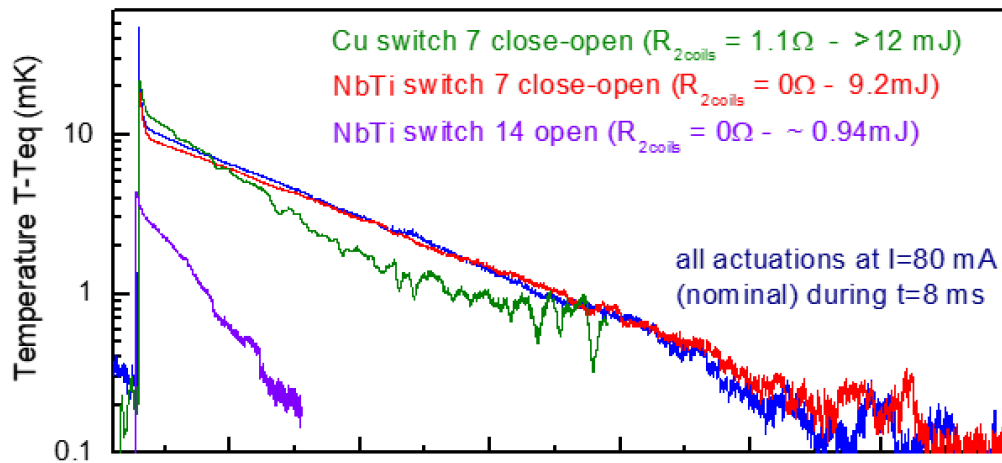


Figure 18 : Refrigerator heating due to several experiments.

The first observation when we compare green and red curves is that the measured dissipated energy when switching with non-superconducting coils is 10%-15% higher than with superconducting coils, thus confirming that Joule effect in the coil is a minor cause of heating. We found that 85% of the energy is not burnt in coil resistance.

Then, the second observation, when applying the same electrical pulses in a direction that does not switch the actuator, the dissipated power is 10 times smaller than when the actuator switches when we compare red and violet curves. This again shows that the main source of dissipation comes from the mechanical actuator and kinetic energy.

The conclusion is that NbTi-Cu coils do not bring any advantage to the cryogenic RF switches.

RF parameters at cryogenic temperature

Insertion loss on RF coaxial switches fitted with SMA type connectors can be modeled using “conductor loss” β_1 and “dielectric losses” β_2 .

$$A = \beta_1 + \beta_2$$

$$\beta_1 \text{ (dB/cm)} = \text{Conductor Loss} = \frac{0,274}{Z_c} \left(\frac{\sqrt{\mu_1}}{a \sqrt{\sigma_1}} + \frac{\sqrt{\mu_2}}{b \sqrt{\sigma_2}} \right) \sqrt{F}$$

$$\beta_2 \text{ (dB/cm)} = \text{Dielectric Losses} = 0,91 \cdot \sqrt{\varepsilon} \cdot \tan \delta \cdot K \cdot F \cdot 10^{-3}$$

Where:

Z_c : Characteristic impedance (Ohms)

a : Outer conductor inside diameter (cm)

b : Inner conductor diameter (cm)

F : Frequency (MHz)

σ_1 : Conductivity of inner conductor ($\Omega \cdot \text{cm}$)⁻¹

σ_2 : Conductivity of outer conductor ($\Omega \cdot \text{cm}$)⁻¹

μ_1 : Magnetic permeability of inner conductor

μ_2 : Magnetic permeability of outer conductor

ε : Dielectric constant

$\tan \delta$: Loss tangent

K = Ratio between the two conductor's b/a

The composite Insertion Loss of a transmission line is determined by the losses associated with the inner and outer conductors, the dielectric medium and characteristic impedance mismatches.

At cryogenic temperature conductor loss is neglected due to superconductivity. Figure 19 shows the RF characteristic of an RF Ramses switch installed on 10K stage of cryostat.

Temperature monitors were attached directly to RF body of Ramses SP6T switch. RF performances were tested in-situ.

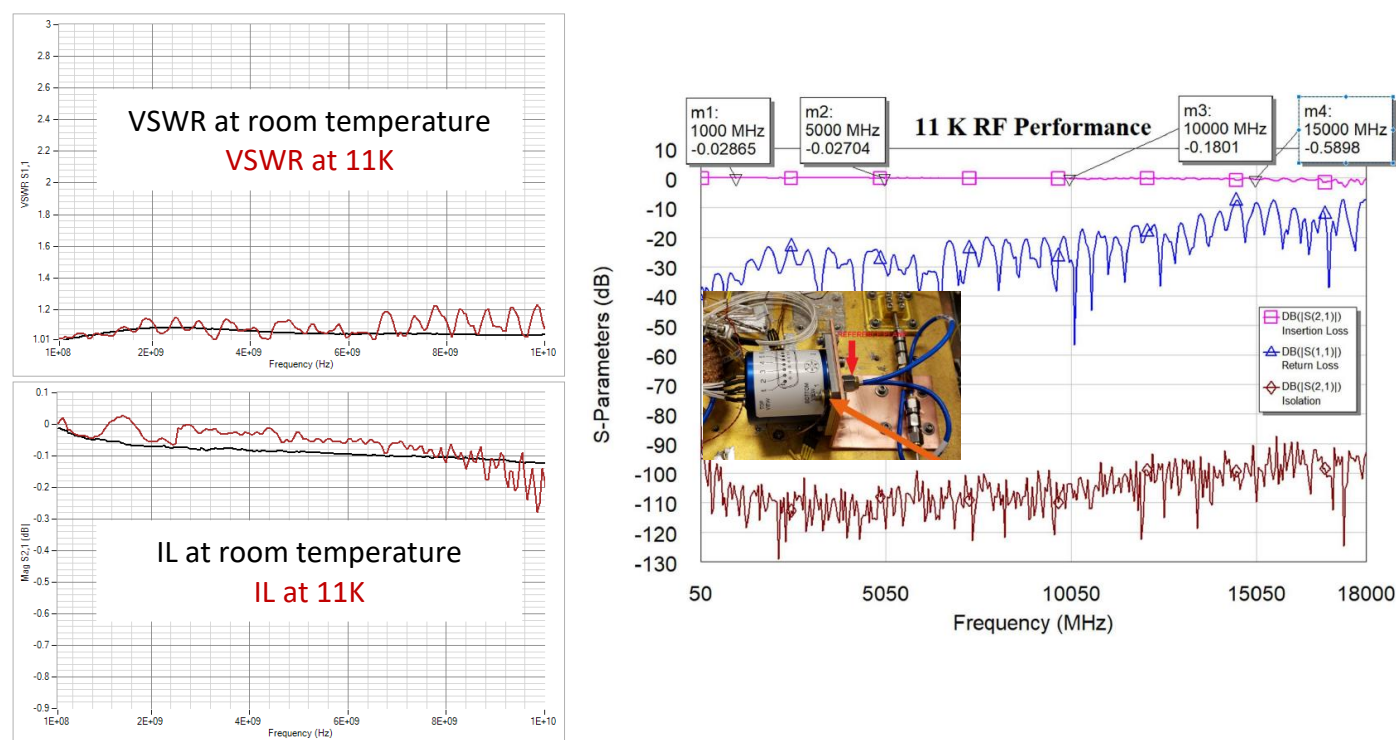


Figure 19 : Cryogenic RF performance at 11K.

Figure 20 shows the maximum insertion loss at 300K and 50mK at several frequencies on a Ramses cryogenic SP6T switch.

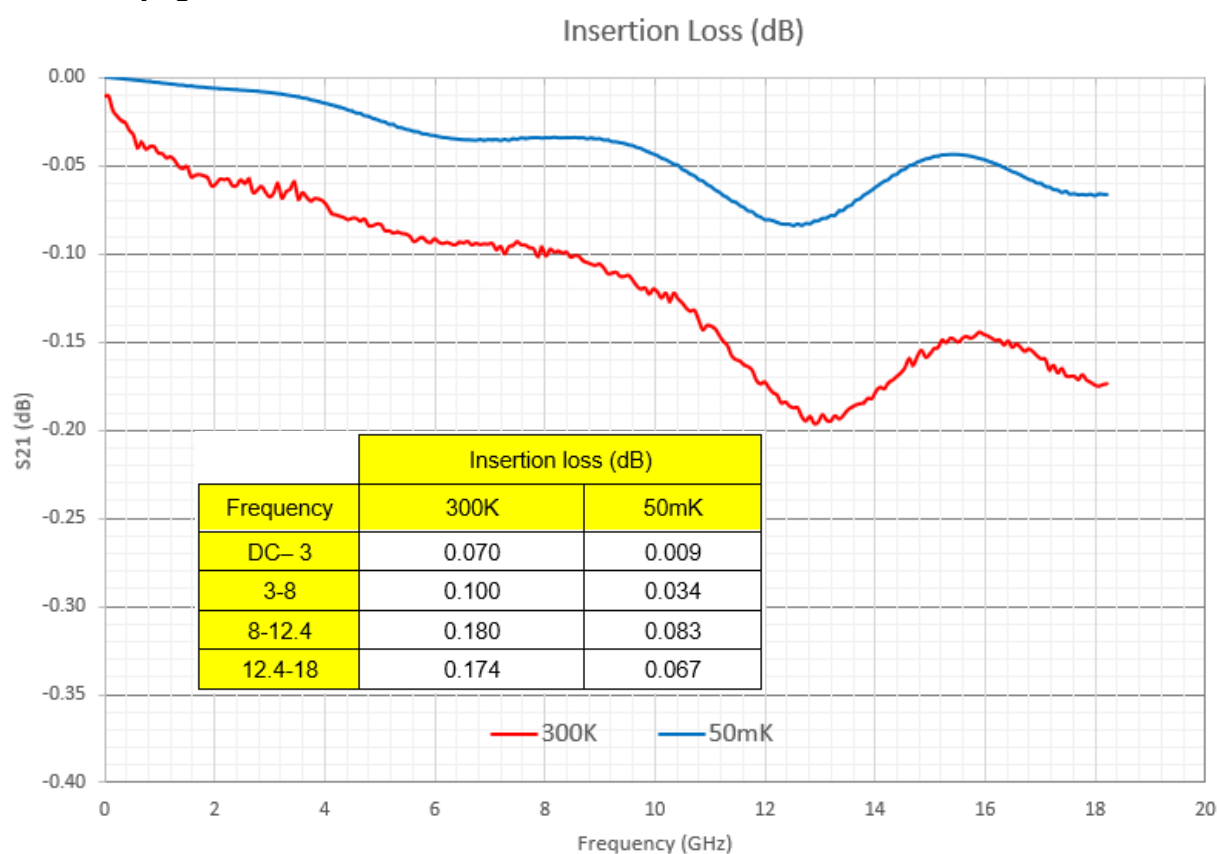


Figure 20 : Cryogenic RF performance at 300K and 50mK.

RF repeatability and dispersion

Radiall has improved the life expectancy and reduced size of the switches. On the subminiature SP6T series, the attachment of the only moving part of the actuator on two parallel cantilever beams suppresses the friction surfaces between the housing and the moving parts of the actuator. This improvement associated with the mounting of the second moving part suspended between the two spring blades eliminates all friction inside of the Ramses switches.

The main difference between the Ramses design and a classic design is its electrical life expectancy. The Ramses design allows users to perform life tests successfully beyond several million switching cycles without RF contact resistance failure or switching time variation over the entire operating temperature range. The particular suspension system ensures strong steady contact force, perfect geometric positioning of the RF blade into the RF line, and exceptional contact cleanliness switching cycle after switching cycle. Repeatability test campaigns performed on subminiature SP6T series have demonstrated standard deviation repeatability results up to 10.000.000 switching cycles. See table below.

Frequency	Insertion loss		V.S.W.R.
	Magnitude (dB)	Phase (°)	
DC– 26.5	0.035 dB	0.98°	0.037

Figure 21 shows curves in 3D illustrate the RF characteristics over the entire life span guaranteed into the technical data sheet at ambient temperature.

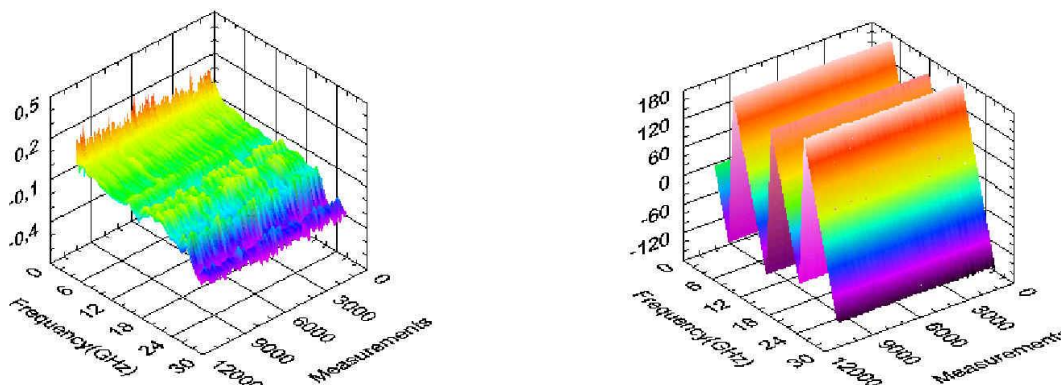


Figure 21: Insertion loss in magnitude and phase over 10 million switching cycles

For applications which need to use a VNA to calibrate at cryogenic temperature, Radiall RF switches have good repeatability and consistency among the channels. Figure 22 shows that the electrical length variation is lower than 1ps from DC up to 18GHz.

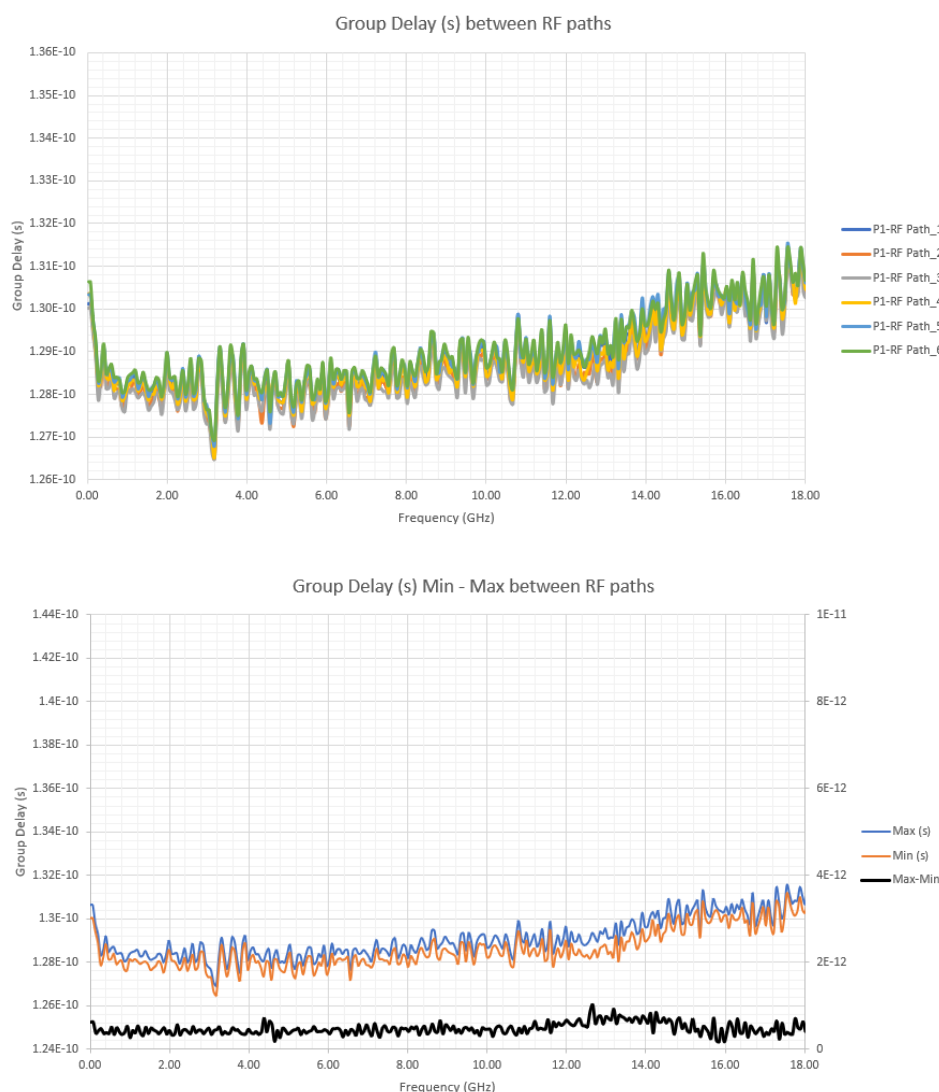


Figure 22: Electrical length variation (Group Delay) on 6 RF paths from DC up to 18GHz